MAUSAM, **77**, 2 (April 2026), 527-540

MAUSAM

DOI: https://doi.org/10.54302/mausam.v77i2.6738
Homepage: https://mausamjournal.imd.gov.in/index.php/MAUSAM

UDC No.551.515.2:551.511 (267.64)

Thermodynamic behaviors associated with the intensity of Tropical Cyclone in the Bay of Bengal

KH. HAFIZUR RAHMAN[1,2*] and M. A. TAHER[1]

[1]*Department of Mathematics, Dhaka University of Engineering & Technology, Bangladesh*

[2]*Bangladesh Meteorology Department, Agargaon, Dhaka, Bangladesh*

(*Received 13 July 2024, Accepted 19 September 2025*)

***Corresponding author's email: rs77_hafizbmd@yahoo.com**

सार – उष्णकटिबंधीय चक्रवात (टीसी) सबसे विनाशकारी प्राकृतिक आपदाओं में से एक हैं, जिसके परिणामस्वरूप अक्सर महत्वपूर्ण मानवीय हताहत और आर्थिक नुकसान होता है। इन प्रतिकूल प्रभावों को कम करने के लिए सटीक पूर्वानुमान और प्रारंभिक चेतावनी महत्वपूर्ण हैं। यह अध्ययन वेदर रिसर्च एंड फोरकास्टिंग (डब्ल्यूआरएफ) मॉडल का उपयोग करके हीट फ्लक्स, उष्णकटिबंधीय चक्रवात की गर्म केंद्र संरचना और तीव्रता के साथ संबंध का मूल्यांकन करता है, जिसमें तीन उल्लेखनीय चक्रवातों पर ध्यान केंद्रित किया गया है: अम्फान (2020), बुलबुल (2019), और तितली (2018)। मॉडल को सीमा और प्रारंभिक स्थितियों के लिए ग्लोबल डेटा एसिमिलेशन प्रणाली (जीडीएएस)/फाइनल एनालिसिस (एफएनएल) डेटा के साथ शुरू किया गया। अनुकरणित हीट फ्लक्स, गर्म केंद्र संरचना और उष्णकटिबंधीय चक्रवात तीव्रता को पुन: विश्लेषण और सर्वश्रेष्ठ मार्ग डेटासेट के साथ मान्य किया गया। परिणाम दर्शाते हैं कि डब्ल्यूआरएफ मॉडल प्रभावी रूप से हीट फ्लक्स, गर्म केंद्र विशेषताओं और चयनित उष्णकटिबंधीय चक्रवात की तीव्रता के साथ संबंध को पुनरुत्पादित करता है, जो उष्णकटिबंधीय चक्रवात अनुसंधान और पूर्वानुमान में इसकी उपयोगिता को रेखांकित करता है।

ABSTRACT. Tropical cyclones (TCs) are among the most destructive natural hazards, often resulting in significant human casualties and economic damage. Accurate forecasting and early warnings are crucial for minimizing these adverse impacts. This study evaluates the heat flux, warm core structure of TCs, and relationship with intensity using the Weather Research and Forecasting (WRF) model, focusing on three notable cyclones: Amphan (2020), Bulbul (2019), and Titli (2018). The model was initialized with Global Data Assimilation System (GDAS)/Final Analysis (FNL) data for boundary and initial conditions. The simulated heat flux, warm core structure, and TC intensity were validated against reanalysis and best track datasets. The results demonstrate that the WRF model effectively reproduces heat flux, warm core characteristics, and the relationship with the intensity of the selected TCs, underscoring its utility in TC research and forecasting.

Key words – Tropical cyclones, WRF model, Bay of Bengal, Latent heat flux, Heat map.

1. Introduction

Tropical cyclones (TCs) are among the most destructive atmospheric phenomena on Earth. The countries bordering the Bay of Bengal (BoB), especially Bangladesh and India, are among the most severely affected regions in the world. The nations surrounding the BoB basin experience nearly 7% of all global TCs (Mondal *et al.,* 2022). Most TCs originate over the BoB and land on the east coasts of India and Bangladesh.

The introduction of the Numerical Weather Prediction (NWP) model has significantly improved the prediction of TCs in terms of their tracks and intensities. However, accurate TC prediction remains a challenge for operational forecasters. High-resolution mesoscale models, combined with quality data assimilation methods and suitable parameterization schemes, have been widely used to understand the behavior of TCs in the North Indian Ocean (NIO) (Chandrasekar and Balaji, 2016; Mahala *et al.,* 2015a; Reddy *et al.,* 2014; Gopalakrishnan *et al.,* 2013; Osuri *et al.,* 2011).

In recent years, advancements in computing facilities, improved implementation of physical processes, enhanced observational capabilities, and advanced data

assimilation methods have significantly improved the performance of NWP models (Routray *et al.,* 2019; Tiwari *et al.,* 2019). The WRF model's performance has been assessed across various oceanic basins (Mugume *et al.,* 2017; Osuri *et al.,* 2013; Srinivas *et al.,* 2013), and it has demonstrated reasonable capability in simulating TCs. Notably, a case study evaluated the WRF model's performance in simulating the VSCS Titli (Mahala *et al.,* 2019) and found it reasonably effective for TC simulation. The warm-core structure of TC plays a crucial role in its intensification and overall dynamics. Several studies using satellite remote sensing data have investigated this relationship, particularly over the Atlantic and Pacific Ocean basins. These studies consistently indicate a positive correlation between the strength of the warm core and the rate of TC intensification, as well as a positive association between the vertical extent (height) of the warm core and the overall TC intensity (Komaromi & Doyle, 2017; Chen & Zhang, 2017; Wang *et al.,* 2020). In contrast, research focusing on the Bay of Bengal (BoB) remains limited, with only a few notable contributions (Raju *et al.,* 2012; Singh *et al.,* 2021). Consequently, the applicability and robustness of the observed warm-core intensity relationships in the BoB region remain inadequately validated. High-resolution simulations using the WRF model can help us better understand warm-core systems in this region. This research is crucial for improving TC intensity predictions and strengthening disaster preparedness efforts. Therefore, this study investigates key thermodynamic parameters, particularly the warm-core structure, and their relationship with TC intensity over the BoB.

1.1. Overview of selected TCs

1.1.1 *Amphan*

The Super Cyclonic Storm (SuCS) Amphan originated from the remnants of a low-pressure area linked to an equatorial easterly wave over the south Andaman Sea and adjoining southeast BoB on May 13, 2020. By May 14, it became a well-marked low-pressure system over the southeast BoB. Favorable atmospheric conditions led to its development into a depression (D) in the early hours of May 16, which intensified into a deep depression (DD) later that day (0900 UTC). Moving north-northwestward, it became Cyclonic Storm (CS) Amphan by 1200 UTC on May 16. It further intensified into a Severe Cyclonic Storm (SCS) by 0300 UTC on May 17, a Very Severe Cyclonic Storm (VSCS) by 0900 UTC, and an Extremely Severe Cyclonic Storm (ESCS) by 2100 UTC. Rapid intensification led to SuCS status by 0600 UTC on May 18 over the west-central BoB. Amphan maintained this intensity for nearly 24 hours before weakening into an ESCS by 0600 UTC on May 19. Approaching the coast, it made landfall as a VSCS near the Sundarbans (West Bengal–Bangladesh border) between 1000 and 1200 UTC on May 20 with peak winds of 85 knots, gusting to 100 knots. It weakened steadily thereafter, becoming a depression over northern Bangladesh by May 21 (RSMC, New Delhi, 2021).

1.1.2. *Bulbul*

The VSCS Bulbul originated from the remnants of Tropical Storm Matmo (28 Oct–2 Nov 2019) over the West Pacific, which later re-emerged into the North Andaman Sea. A low-pressure area developed over the North Andaman Sea early on 04 Nov (0000 UTC), intensifying into a well-marked low by afternoon on the same day. Under favorable environmental conditions, it strengthened into a D over the east-central and adjoining southeast BoB by 0000 UTC on 05 Nov and into a DD by 0000 UTC on 06 Nov. Continuing its north-northwestward movement, it became CS Bulbul by 1800 UTC on 06 Nov. Further intensification occurred as it moved over the west-central and adjoining east-central BoB, becoming a SCS by 1200 UTC on 07 Nov and a VSCS by 0000 UTC on 08 Nov. Bulbul maintained a northward track until 0900 UTC on 09 Nov, then began to re-curve northeastward. It weakened into an SCS before making landfall along the West Bengal coast near the Sundarbans between 1500 and 1800 UTC on 09 Nov with winds of 60 knots, gusting to 70 knots. Moving northeastward, it weakened into a CS, then into a DD and a depression over southeast Bangladesh by 11 Nov (RSMC, New Delhi, 2020).

1.1.3. *Titli*

The VSCS Titli originated from a low-pressure area over the southeast BoB and adjoining north Andaman Sea around 0300 UTC on 07 Oct 2018. It intensified into a D over the east-central BoB by 0300 UTC on 08 Oct, and further into a DD around 1800 UTC the same day. Continuing to strengthen, the system developed into CS Titli by 0600 UTC on 09 Oct. Moving northwestward, it intensified into a SCS by 0300 UTC on 10 Oct and further into a VSCS by 0600 UTC the same day. VSCS Titli continued its path toward the Indian coastline and made landfall over the north Andhra Pradesh and south Odisha coasts around 0000 UTC on 11 Oct 2018, with estimated maximum sustained winds of 80 knots. Notably, the system retained its cyclonic storm intensity for approximately 15 hours after landfall, an unusual feature over land, before gradually weakening. The persistence of Titli's intensity post-landfall highlights its structural resilience and potential for extended inland impacts (RSMC, New Delhi, 2019).

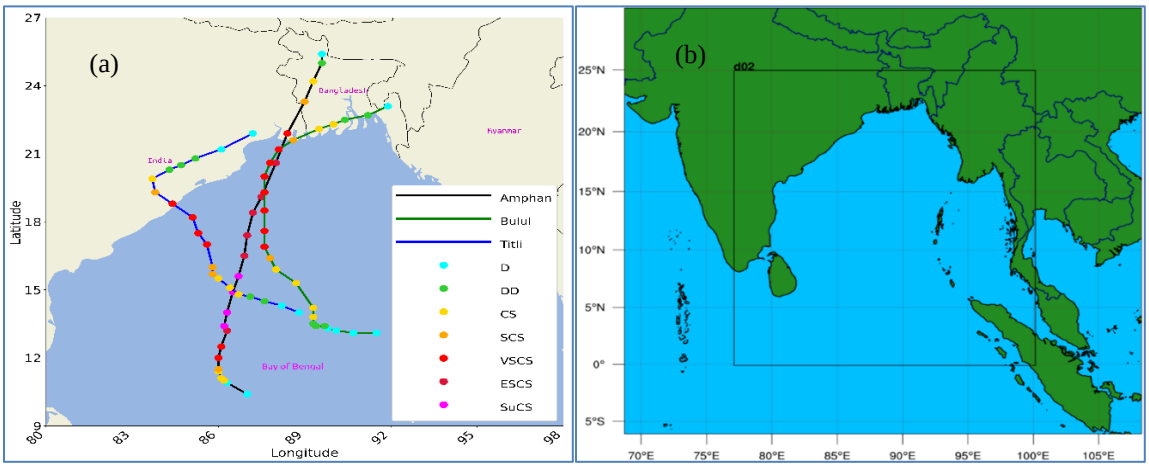

Figs. 1(a&b). (a) Estimated track of the selected TC and (b) Model domain for the study.

2. Data and Methodology

2.1 *Numerical Simulations*

The present study used the non-hydrostatic compressible Advanced Research Weather Research and Forecasting (WRF-ARW) v.4.2, developed by the National Center for Atmospheric Research (NCAR). The WRF is configured with two two-way interactive nested domains with horizontal resolutions of 27 km, 9 km, and 42 vertical levels with model top at 10 hPa. The inner 9 km resolution domain covers the BoB and the adjacent mainland areas. All the simulations are initialized at the depression stage according to the RSMC best track data. The model is integrated up to dissipation to the depression stage after the landfall.

The initial and boundary conditions for the model are obtained from the Global Tropospheric Analyses and Forecast Grids data, which have a resolution of 0.25°× 0.25°, sourced from the GDAS/FNL dataset provided by the National Centers for Environmental Prediction (NCEP). While the Sea Surface Temperature (SST) is maintained as a constant value throughout the integration, the lateral boundary conditions are updated at 6-hour intervals. The United States Geological Survey (USGS) 10-minute resolution terrain information has been employed as topographical data in the WRF Preprocessing System (WPS). The technical description of the WRF model is given in Samarock *et al*. (2019). The input parameters & details for the model are provided in Table 1. The selected domain for the study is illustrated in Fig. 1.

2.2. *Observation/reanalysis data sets*

The simulation results are evaluated by comparing them with best track data and reanalysis datasets from various sources. Specifically, the simulated minimum Mean Sea Level Pressure (MSLP) and Maximum Sustained Wind (MSW) are compared with best track estimates provided by the Regional Specialized Meteorological Centre (RSMC), New Delhi. To assess the performance of the WRF model, data from the ERA5 reanalysis, developed by the European Centre for Medium-Range Weather Forecasts (ECMWF), are used. Additionally, the warm core temperature deviation and the height of the warm core are evaluated against ERA5 data.

3. Results and discussion

This section presents model-simulated fields related to TC intensity, including MSLP, MWS, and the warm-core structure, along with associated intensity variations. The simulations were initialized at various forecast lead times (*i.e*., 120, 96, 72, 48, and 24 hours). Since longer lead times are critical for effective disaster preparedness and response, particular attention is given to the 120-hour forecast to evaluate the model's ability to reproduce the thermodynamic characteristics related to changes in TC intensity.

3.1. *Observed and simulated MSLP and MSW*

The intensity of a TC is typically assessed using two key parameters: the MWS and the minimum MSLP. The evolution of intensity of selected TCs were captured through comparisons among the best track data, ERA5 reanalysis, and model simulations. The model-simulated, best track, and ERA5-derived MWS and minimum MSLP based on the 0000 UTC 16 May initial condition for Amphan are presented in Fig. 2. The best track analysis showed a minimum MSLP of approximately 920hPa and MSW of around 130 knots at peak intensity on 1800 UTC May 18. In comparison, the ERA5 reanalysis strongly underestimated the intensity, showing a minimum MSLP pressure around 943hPa and MSW near 67 knots on 0900

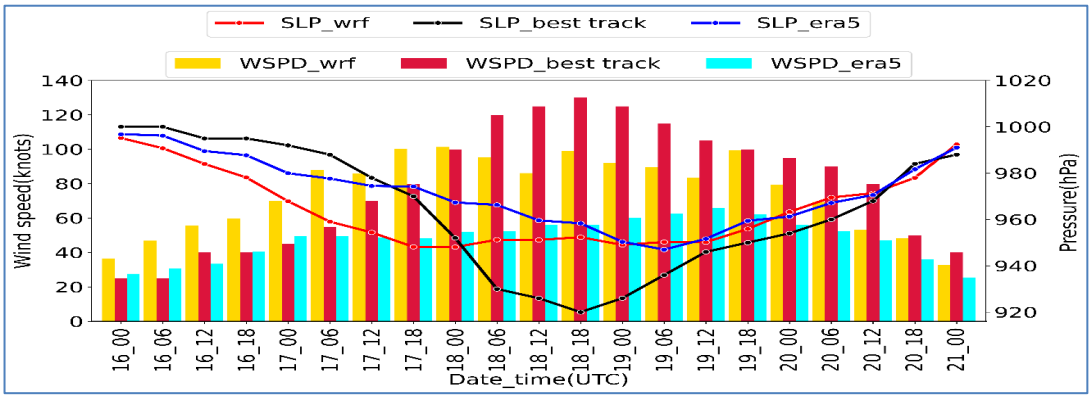

Fig. 2. Best track and model simulated minimum MSLP and MSW for Amphan. The vertical bars represent MSW, where cyan represents the best track and green represents the model-predicted wind speed. The horizontal lines represent minimum MSLP, where black represents the best track minimum MSLP and red represents the model-predicted

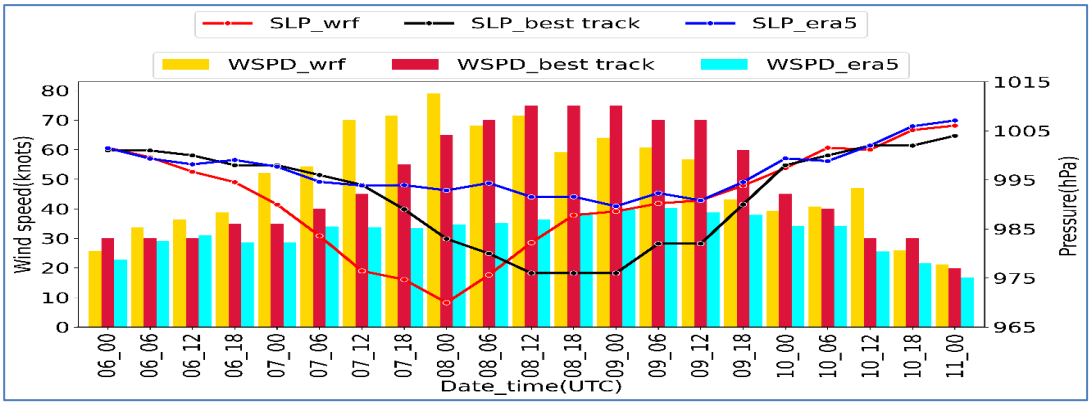

Fig. 3. Best track and model simulated minimum MSLP and MSW for Bulbul. The vertical bars represent MSW, where cyan represents the best track and green represents the model-predicted wind speed. The horizontal lines represent minimum MSLP, where black represents the best track minimum MSLP and red represents the model-predicted.

TABLE 1

Brief description of WRF model configuration

Model	WRF V4.2
Max_domain	2
Map Projection	Mercator
Resolution	27 km, 9 km
Time step	108s,36s
Central point of the domain	17.5^0 N, 87.5^0E
No. of grid points	152, 265(WE); 144, 298(NS)
No. of Vertical levels	42 Sigma Levels
Horizontal Grid	Arakawa C Grid
Time Integration	Runge-Kutta second and third-order time
Radiation Scheme	Dudhia's short-wave/RRTM long-wave
PBL Scheme	YSU scheme
Convection	Kain-Fritsch (new Eta) scheme
Micro Physics	WSM3-class simple ice scheme

UTC May 19 (Dulac *et al*., 2022). Model simulations initialized at a 120-hour lead time reasonably reproduced the intensity trend but exhibited a slightly weaker system, with a minimum MSLP of about 947 hPa and MSW around 110 knots on 2100 UTC May 17. However, Amphan demonstrated a dynamic intensity evolution, including a rapid intensification phase in its lifetime. Accordingly, it intensified into a VSCS, with MSW 65 knots by 0900 UTC of 17 May, and into a SuCS with the MSW 120 knots around 0600 UTC of 18 May (RSMC, New Delhi, 2020). The WRF simulation also predicted rapid intensification, though there is a temporal deviation of 15 hours, with MSW 60 knots at 1800 UTC on 16 May to MSW of 100 knots at 1800 UTC on 17 May. The slight underestimation could be attributed to model resolution and representation of air-sea interaction processes. However, the model showed poor agreement with the timing and location of peak intensity, indicating its potential reliability for forecasting intense TC like Amphan.

The intensification of Bubul was weaker compared to Amphan, but it still exhibited notable characteristics. The model-simulated best track and ERA5-derived MWS and minimum MSLP based on the 0000 UTC 06 Nov initial condition for Bulbul are presented in Fig. 3. The

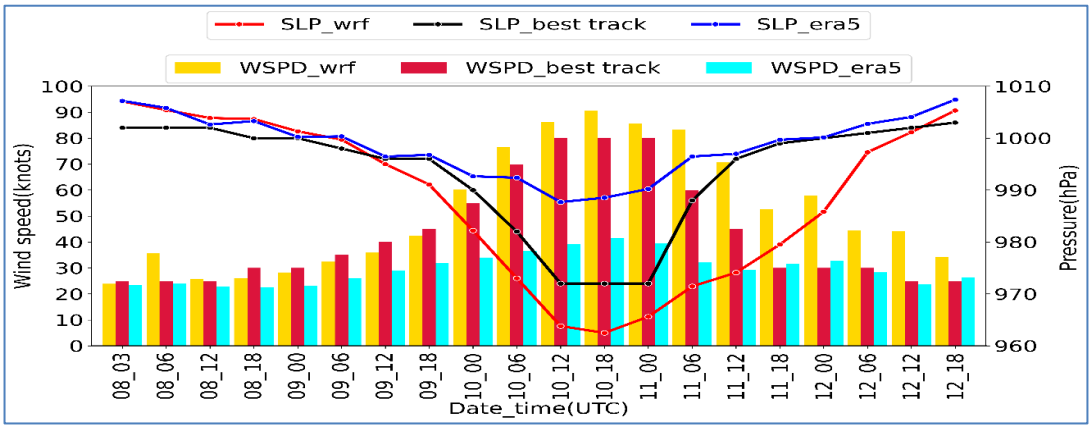

Fig. 4. Best track and model simulated minimum MSLP and MSW for Titli. The vertical bars represent MSW, where cyan represents the best track and green represents the model-predicted wind speed. The horizontal lines represent minimum MSLP, where black represents the best track minimum MSLP and red represents the model-predicted

best track data indicated a minimum MSLP of 976 hPa and MSW of 75 knots at its peak on 1200 UTC Nov 08, 2019. ERA5 reanalysis suggested a slightly higher central pressure around 990 hPa and lower MSW values of about 40 knots on 0000 UTC Nov 09, reflecting ERA5's tendency to smooth extreme intensities. The WRF model simulation captured the general trend but showed a slight overestimation of the peak intensity 12 hours ahead of the best track estimation. The model simulated a minimum MSLP of 976hPa and a peak MSW of 87 knots on 0900 UTC Nov 08, indicating that the model showed stronger low-level winds than estimated. This overestimation suggests that the model may have enhanced convection and latent heat release, contributing to the intensified simulated core. Nevertheless, the evolution of intensity trends remained consistent with observational estimates.

TC Titli exhibited a dynamic intensity evolution, including a rapid intensification phase before landfall. The model-simulated, best track, and ERA5-derived MSW and minimum MSLP based on the 0000 UTC 08 Oct initial condition for Titli are presented in Fig. 4. The best track records noted a minimum MSLP of approximately 972 hPa and MSW of 80 knots at 1200 UTC Oct 10. ERA5 illustrated a minimum MSLP close to 987 hPa with MSW near 43 knots on 2100 UTC Oct 10, again indicating a strong underestimation. The WRF model simulation generated a minimum MSLP of about 963 hPa and MSW around 94 knots on 1500 UTC Oct 10, showing reasonable agreement with observations, though the lead time is 96 hours. The simulation smartly captures the rapid intensification phase with an increase in MSW speed from 52 knots at 2100 UTC on 09 Oct to 86 knots at 1200 UTC on 10 Oct, consistent with best track analysis. The temporal alignment of the simulated peak intensity with the best track data was accurate, and the spatial structure of the storm was also well represented. The model's slight overestimation may reflect limitations in convective parameterization and boundary layer processes, yet it still provides valuable insights into the system's dynamics. Besides, the persistence of cyclonic intensity after landfall can be attributed to favorable thermodynamic conditions over land, particularly the presence of high soil moisture and latent heat fluxes from saturated surfaces, which helped sustain convection and energy supply even after oceanic heat input ceased (Andersen and Shepherd, 2014). Additionally, the proximity to the coast and relatively slow weakening of the low-level inflow allowed the cyclone's inner core to remain organized for an extended period. Warm mid-level temperatures and high atmospheric moisture content also contributed to maintaining a quasi-barotropic warm-core structure, delaying the cyclone's decay. These aspects are consistent with previous studies that suggest land-surface interactions and environmental humidity can significantly influence the post-landfall evolution of tropical cyclones.

3.2 *Warm core structure*

Organized thunderclouds surrounding the center of TCs play a pivotal role in forming the warm core within these systems. The air parcels rising within thunderstorm updrafts are initially very warm and moist as they evaporate from warm tropical oceans. As these parcels ascend and cool, they undergo condensation to form thunderclouds. This condensation process releases energy to the surrounding air, known as the latent heat of condensation. Consequently, the latent heat keeps the air parcels within the TC warmer than their surroundings, maintaining a warm core within the storm.

The release of latent heat is the main contributor to the warm core of a TC, although it is not the only factor. The air within the thunderstorm updrafts spreads outward and flows away from the storm center as it reaches the top of the TC. This outward flow creates divergence aloft,

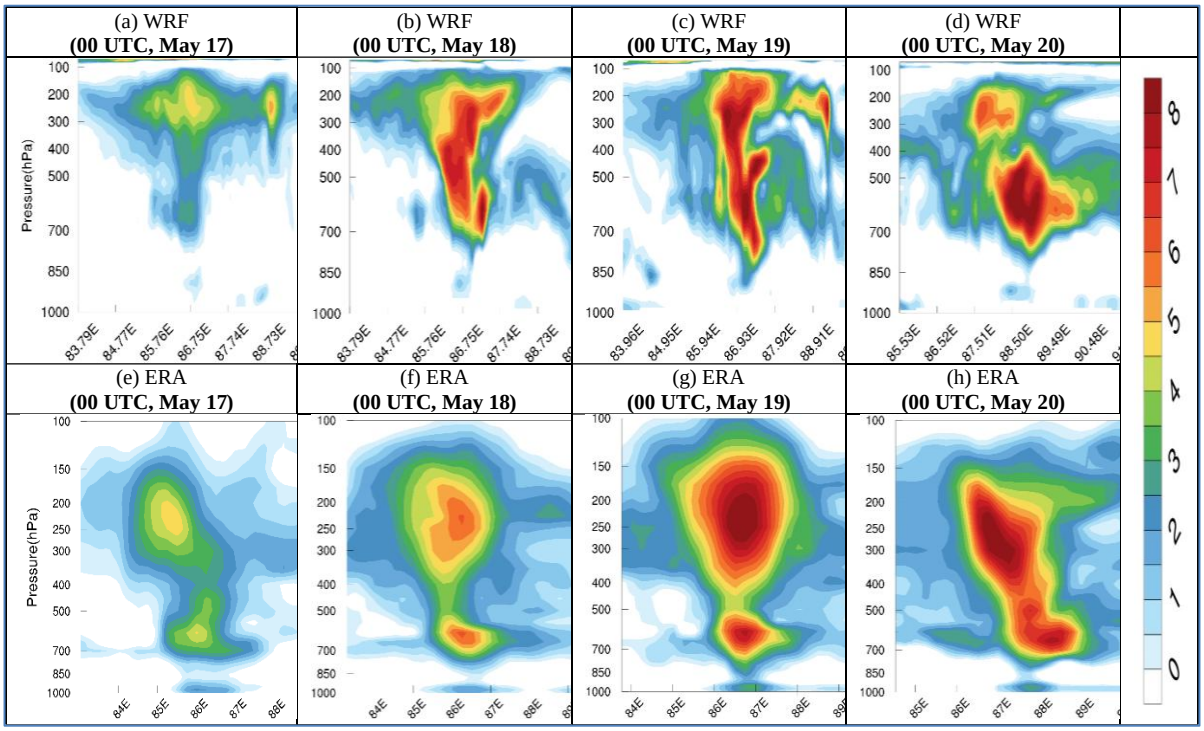

Figs. 5(a-h). Vertical cross-section of temperature deviation (in °C) along the east-west direction through the center of Amphan. (a-d) the model predicted and (e-h) ERA5 reanalysis, valid for (a, e) 00 UTC, 17 May; (b, f) 00 UTC, 18 May; (c, g) 00 UTC, 19 May and (d, h) 00 UTC, 20 May, based on 00 UTC 16 May initial condition

reducing the weight of air columns near the storm center and decreasing sea-level pressure. Nevertheless, some air remains near the top of the storm and descends over the storm's center. As this air descends, it warms due to compression in the higher-pressure environment. The warm core of a TC results from the sinking and warming of air over the storm's center. This warm core enhances the TC's intensity because the warmer air columns in the storm's center are less dense, further reducing central pressure.

The warm core structure is a critical feature of TCs, often described in terms of two common parameters: strength and height. The maximum temperature deviation determines the strength of a warm core, while the height indicates the vertical level at which the maximum temperature deviation is observed. Previous studies have suggested that the height of the warm core exhibits no significant positive correlation with TC intensity, whereas the warm core's strength is positively correlated with TC intensity (Wang and Jiang, 2019; Ohno *et al.*, 2016).

Fig. 5-7 presents the vertical cross-section of temperature deviation along the east-west direction through the center of selected TCs. Temperature deviations are calculated by subtracting the time-averaged temperature values from the values at each forecast hour.

It is evident from Fig. 5 that at 0000 UTC on May 17, the temperature deviation spreads horizontally between the 300-200 hPa levels, with core values 4-5°C, above the TC center, at the same time there is secondary core near 700hPa above the center with core value 3°C (Fig. 5a) . Corresponding ERA5 reanalysis data exhibit a similar signature, core is more defined, but the secondary core is stronger than the simulated one, although there are some spatial deviations (Fig. 5e). As the system underwent rapid intensification, at 0000 UTC on May 18, the central region of the TC showed a positive temperature deviation, the warm core extending vertically between 700-200 hPa, with strong temperature strong deviation. The secondary core also intensified near 700 hPa (Fig. 5b). As the system retains its intensity, the warm core is tightly confined vertically due to strong updrafts and intense latent heat release near the center. Similar signatures are present in the corresponding ERA5 reanalysis (Fig. 5f). By 0000 UTC on May 19, the warm core became more distinct, extending vertically downward. The primary core lies between the 300-200 hPa levels with core value 8 °C, and the secondary core intensifies further near 700 hPa (Fig. 5c). A Similar signature is present in ERA5 reanalysis, two separated warm cores exist. The upper level core is stronger than the lower level near 700hPa and expanded vertically between 400-150hPa with core value between 300-200 hPa (Fig. 5g). The system continued to weaken gradually as it

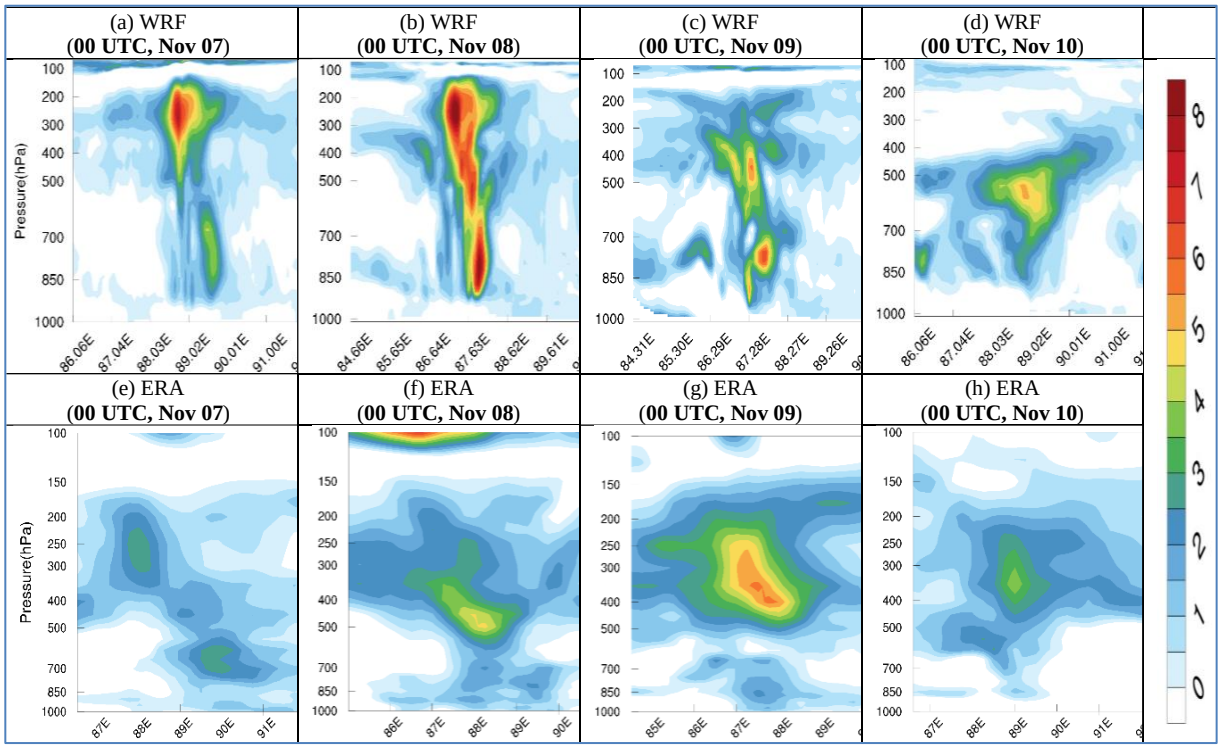

Figs. 6(a-h). Vertical cross-section of temperature deviation (in °C) along the east-west direction through the center of Bulbul. (a-d) the model predicted and (e-h) ERA5 reanalysis, valid for (a, e) 00 UTC, 07 Nov; (b, f) 00 UTC, 08 Nov; (c, g) 00 UTC, 09 Nov and (d, h) 00 UTC, 10 Nov, based on 00 UTC 10 Nov initial condition

approached the coastline. By 0000 UTC on May 20, the upper-level warm core became weakened, and the lower-level warm core between 700-500 hPa expanded horizontally, with the vertical alignment of the warm core tilted (Fig. 5d). Corresponding ERA5 reanalysis represents a similar signature, although the upper-level warm core is stronger than simulated.

The timing of warm core development and compactness with higher temperature deviation in the simulation agreed well with the rapid intensification phase, highlighting that the strength and altitude of the warm core were critical factors influencing the intensity of Amphan. Minor differences in the magnitude of warming between WRF and ERA5 likely contributed to the slight underprediction of the peak intensity. During the intensification stages, it is observed that the position of the warm core within the system varies as the intensity changes, which is consistent with a previous study by Wang *et al*. (2020).

Although Bulbul was less intense than Amphan, it still developed a distinct warm core structure that significantly contributed to its moderate intensification. In the simulations, the WRF model produced a primary warm core anomaly peaking at around 7 °C near 200-300 hPa and a secondary core near 700-800 hPa with a deviation of 3-4 °C (Fig. 6a). ERA5 reanalysis similarly showed two warm cores, although broader and slightly weaker (2-3 °C deviation), and extending to near the same level as the model (Fig. 6e). As Bulbul intensified, the warm core expanded vertically, with both cores distinct and a deviation of about 8 °C (Fig. 6b). The corresponding ERA5 reanalysis illustrated the intensification of the core between 400-500 hPa, with a deviation of 4-5 °C (Fig. 6f). On the following day, the system underwent stages of weakening; the warm cores weakened, and the upper-level core extended vertically down near 400-500 hPa. The lower-level core remained at the same level (700-800 hPa) but was stronger than the upper-level core (Fig. 6c). ERA5 reanalysis depicted some intensification, exhibiting a broader horizontal and vertical extension (Fig. 6g). Further weakening was illustrated by the simulation, with the warm core expanding horizontally and forming a single core near 500-700 hPa (Fig. 6d), a corresponding signature present in the ERA5 reanalysis (Fig. 6h). The correspondence between the warm core height and the moderate intensification phase in both WRF and ERA5 indicates that the model reasonably captured the thermodynamic environment supporting Bulbul's intensity evolution. However, the slight overestimation of warm core magnitude and compactness in the simulation likely led to a minor overprediction of Bulbul's peak intensity

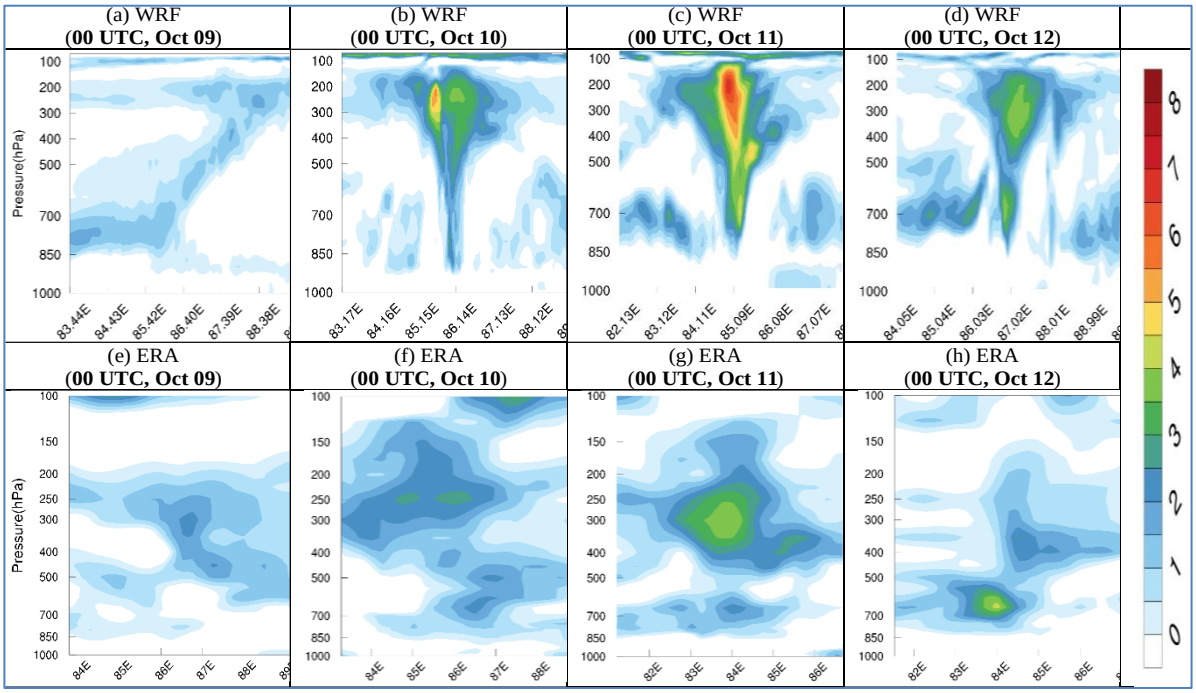

Figs. 7(a-h). Vertical cross-section of temperature deviation (in °C) along the east-west direction through the center of Titli. (a-d) the model predicted and (e-h) ERA5 reanalysis, valid for (a, e) 00 UTC, 09 Oct; (b, f) 00 UTC, 10 Oct; (c, g) 00 UTC, 11 Oct and (d, h) 00 UTC, 12 Oct, based on 00 UTC 08 Oct initial condition

compared to best track estimates. The link between warm core strength, vertical extent, and surface intensity was thus evident but less pronounced than in stronger systems like Amphan. The warm core height in the simulation was fairly consistent with reanalysis, suggesting that while the simulated Bulbul was slightly stronger, its thermal structure was represented reasonably well.

Titli, which underwent a phase of rapid intensification before landfall, the simulation results provided important insights into the role of thermodynamics in intensity change. The WRF model simulation depicted that at 0000 UTC on Oct 09, the temperature deviation is very weak (about 2 °C) and the warm core is not distinct, tilted vertically near 850-200hPa (Fig. 7a). ERA5 reanalysis showed the development of warm core near 300 hPa of about 2 °C deviation (Fig. 7e). The simulation smartly captures the rapid intensification phase with the development of the distinct warm core near 200-300hPa which is vertically extended downward (Fig. 7b), temperature deviation reaches about 7 °C. ERA5 reanalysis depicted further development of warm core near 250 hPa with temperature deviation of (3-4) °C (Fig. 7f). As the system retained its intensity, at 0000 UTC on Oct 10, the central region of the TC showed a positive temperature deviation (about 7 °C), extending vertically between 700-200 hPa, with the warm core concentrated between 200-300 hPa (Fig. 7c). Similar signatures are present in the corresponding ERA5 reanalysis, warm core located near 250-300 hPa, the values tend to be underestimated (about 4.5 °C), as the low TC intensity observed in the ERA5 reanalysis (Fig. 7g). By 0000 UTC on Oct 12, as the system weakened, the warm core became weaker, and the temperature deviation became about 3 °C (Fig 7d). ERA5 reanalysis also showed weakening of the system, while it remained underestimated compared to the model. During the intensification stages, it is observed that the position of the warm core within the system varies as the intensity changes, which is consistent with a previous study by Wang *et al*. (2020).

The alignment of the timing of the peak warm core anomaly with the period of rapid intensification suggests that the model was able to capture the essential thermodynamic processes driving the evolution of Titli. Differences in warm core compactness and vertical structure between WRF and ERA5 likely influenced small inconsistencies in ERA5 reanalysis intensity; nevertheless, the overall consistency of the model reinforces the crucial role of upper-level warming in supporting rapid intensity changes in TCs.

Tropical cyclone intensity is often underestimated in ERA5 primarily due to its relatively coarse spatial resolution (~31 km), which limits its ability to accurately capture the compact inner-core structure of intense cyclones, including the steep pressure gradients and strong

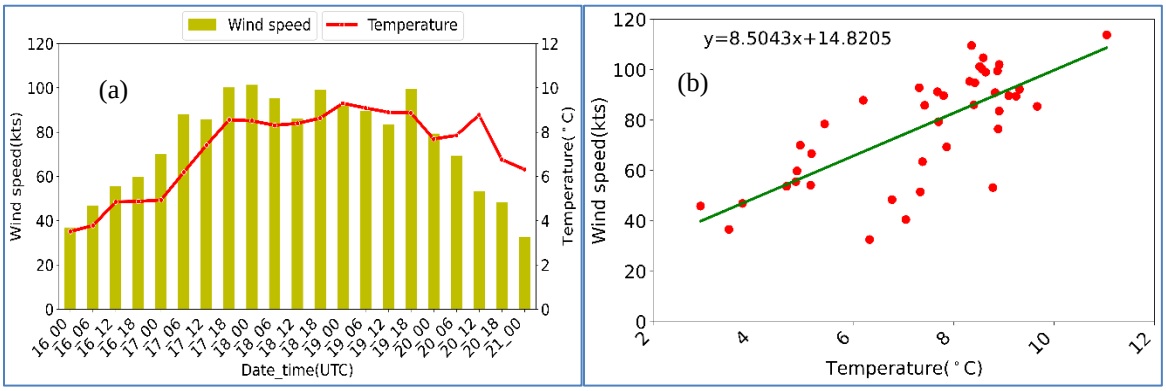

Figs. 8(a&b). (a) Time series analysis of maximum wind speed in knots and mean temperature deviation in °C, (b) Scatter plot of maximum wind speed and mean temperature deviation between 700-200hPa level for Amphan

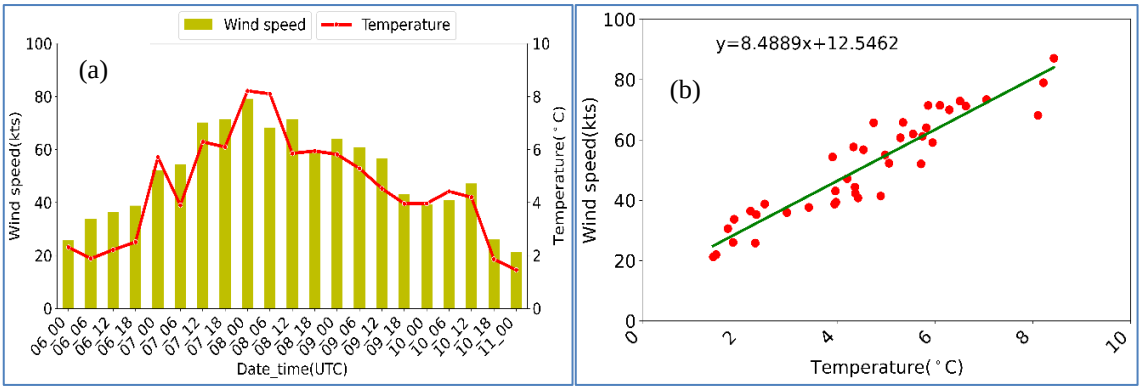

Figs. 9(a&b). (a) Time series analysis of maximum wind speed in knots and mean temperature deviation in °C, (b) Scatter plot of maximum wind speed and mean temperature deviation between 700-200hPa level for Bulbul.

wind maxima near the eyewall. Additionally, ERA5 relies on a global data assimilation system that incorporates a wide range of observations, but these are often sparse over oceanic regions where most TCs develop and intensify. As a result, the strongest phases of intensification, particularly rapid intensification, are often smoothed or delayed. Moreover, ERA5's physical parameterizations are designed for general global applications and may not fully resolve the intense convective processes and diabatic heating that drive rapid cyclone intensification, leading to weaker simulated maximum wind speeds and warm-core anomalies compared to high-resolution models or best-track observations (Dulac *et al*., 2022).

Furthermore, temperature anomalies at various pressure levels are calculated, and the mean temperature deviation is achieved by averaging each value at different pressure levels for selected TCs. A time series analysis and scatter plot of MSW and mean temperature deviation are presented in Fig. 8-10 for the selected TCs.

The time series analysis of MSW and mean temperature deviation during the life cycle of Amphan reveals a strong correlation between upper-level warming and intensification. As Amphan progressed from a cyclonic storm to a super cyclonic storm, the mean temperature deviation between 700-200 hPa increased steadily, indicating the development of a robust warm core. Amphan underwent rapid intensification during its life cycle, and the WRF simulation captures this rapid intensification stage 15 hours prior to the best track estimation. The mean temperature deviation increases from 4.87 °C to 8.56 °C over 24 hours and coincides with the corresponding intensification and peak mean deviation lasting for nearly 48 hours (Fig. 8a). The peak wind speed during the most intense phase coincides with a mean maximum temperature anomaly of approximately 9 °C. The scatter plot further supports this association, showing a near-linear relationship between wind speed and mean temperature deviation, highlighting the thermodynamic influence on storm intensity (Fig. 8b). These results underscore the role of upper-level warming in the rapid intensification of Amphan.

In the case of Bulbul, the time series analysis shows a strong correlation between upper-level warming and intensification, marked by moderate intensification characterized by a gradual increase in maximum wind speed and mid-to-upper tropospheric temperature deviation (Fig. 9a). Bulbul reached peak intensity with

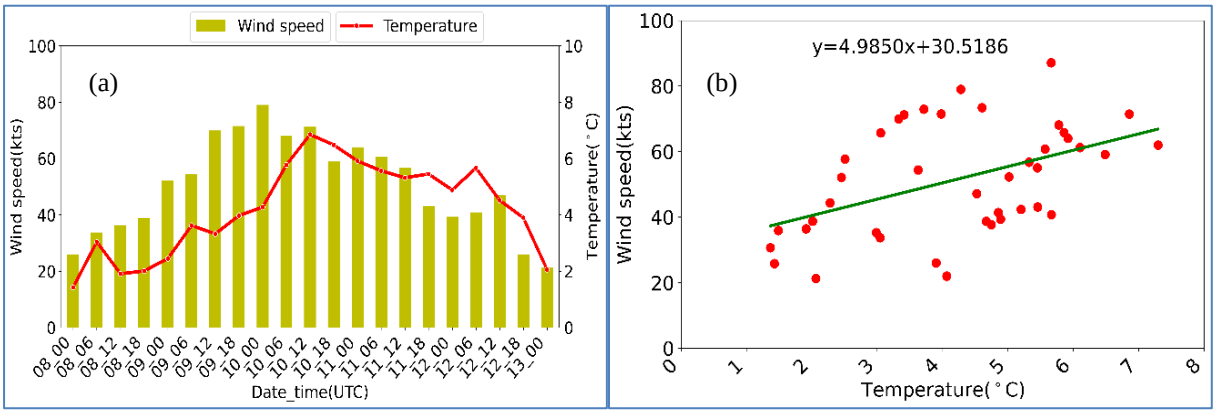

Figs. 10(a&b). (a) Time series analysis of maximum wind speed in knots and mean temperature deviation in °C, (b) Scatter plot of maximum wind speed and mean temperature deviation between 700-200hPa level for Titli

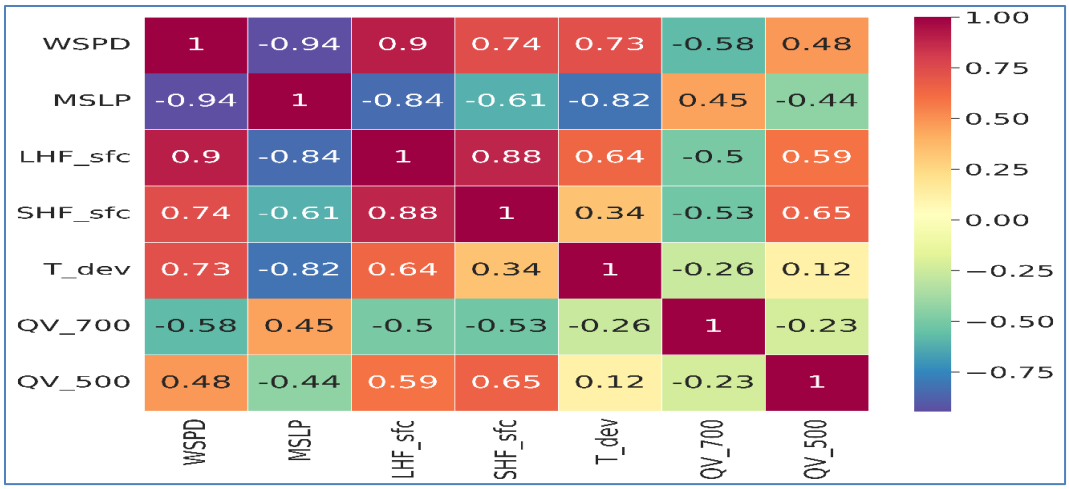

Fig. 11. Heat map representing the correlation matrix of different parameters of Amphan

sustained wind speeds of around 80 knots, accompanied by a peak mean temperature deviation of nearly 8.0 °C in the 700-200 hPa layer at 0000 UTC on 08 Nov, lasting for only 6 hours (Fig. 9a). After that, warm core intensity decreases gradually. The temporal evolution indicates that the storm maintained a warm core structure throughout its lifecycle, though it was weaker than Amphan's. The scatter plot of wind speed versus temperature deviation presents a strong correlation (Fig. 9b), reflecting that while warm core development contributed to Bulbul's intensification, other dynamic factors such as shear and moisture availability also played significant roles.

TC Titli also exhibited a distinctive evolution in its thermodynamic structure. Time series data indicate that maximum wind speed increased rapidly to 90 knots during the intensification phase, accompanied by a rising trend in temperature deviation, peaking at approximately 6.5 °C at 18 UTC on 10 Oct. Titli underwent rapid intensification, and the WRF simulation captures this stage almost simultaneously with the best track estimation. The maximum wind speed rises from 52 knots at 2100 UTC on 09 Oct to 86 knots at 12 UTC on 10 Oct. The mean temperature deviation increases from 3.41 °C to 6.85 °C over 24 hours, coinciding with the corresponding intensification (Fig. 10a). The storm maintained this deviation for several hours after landfall, indicating that a lingering warm core aloft helps the system sustain cyclonic storm intensity for several hours even after landfall. The scatter plot analysis reveals a positive correlation between maximum wind speed and temperature deviation, similar to Amphan and Bulbul, with a greater variability (Fig. 10 b).

3.3 *Heat map*

Heat maps provide a convenient and effective means of summarizing results and visualizing critical components. They are graphical representations of data, presenting values on a two-dimensional grid using colors to signify data intensity relative to one another. The correlation matrices (heat maps) for TCs Amphan, Bulbul,

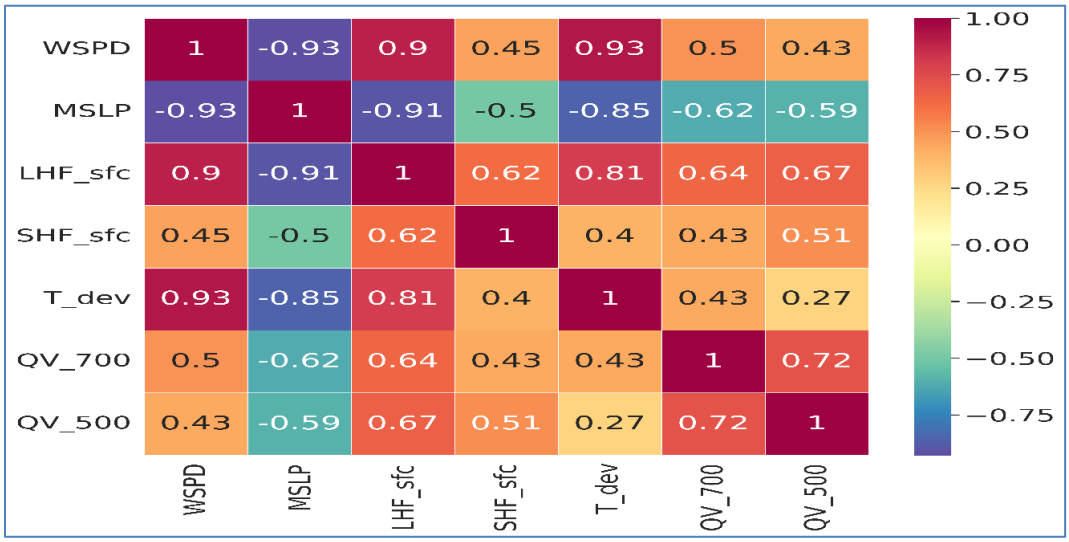

Fig. 12. Heat map representing the correlation matrix of different parameters of Bulbul

and Titli, focusing on the relationships between surface latent heat flux (LHF_sfc), surface sensible heat flux (SHF_sfc), mean temperature deviation (T_dev), water vapor mixing ratio at 700hPa (QV_700) & water vapor mixing ratio at 500 hPa (QV_500), and TC intensity in terms of maximum wind speed and minimum mean sea-level pressure (MSLP), are presented in Fig. 11-13, which show the relationships and influences of different parameters on TC intensity.

Area-average values of these thermodynamic parameters are calculated within a (2^0 x 2^0) grid box surrounding the TC center (minimum MSLP center) at three-hour intervals. TC intensity is typically expressed in terms of MSW, and minimum MSLP values are also determined at three-hour intervals.

A strong correlation is observed between tropical cyclone (TC) intensity, measured by MSW and minimum MSLP, and LHF. Specifically, LHF shows a high positive correlation with MSW (r = 0.90) and a strong negative correlation with minimum MSLP (r = -0.94), suggesting that increased surface evaporation enhances convective activity, thereby intensifying the storm (Fig. 11). In contrast, the correlation between SHF and TC intensity is relatively weaker, with SHF positively correlated with MSW (r = 0.74) and negatively correlated with minimum MSLP (r = -0.61). This weaker relationship is expected, as SHF plays a secondary role in cyclone intensification compared to LHF.

The mean T_dev between 700–200hPa shows a strong negative correlation with minimum MSLP (r = -0.82), implying that greater upper-level warming, driven by intense convection, leads to lower surface pressures. Correspondingly, mean T_dev is positively correlated with MSW (r = 0.73), reinforcing its association with increased TC intensity.

Remarkably, the QV_700 displays a negative correlation with MSW (r = -0.58) and a positive correlation with MSLP, suggesting that excess mid-level moisture may not always enhance intensity. Meanwhile, QV_500 shows a positive correlation with MSW (r = 0.48) and a negative correlation with minimum MSLP, indicating that upper-level moisture supports sustained convection and low surface pressure during storm intensification.

As Amphan underwent rapid intensification and reached SuCS status, the system likely transported moisture efficiently from the lower and mid-levels to the upper levels, resulting in relative drying near the 700 hPa level despite high overall atmospheric humidity (Plotnik *et al.*, 2021). This vertical redistribution of moisture can lead to a decrease in the area-averaged QV at 700 hPa even as the storm intensifies, producing a negative correlation between QV_700 and MSW. Additionally, strong cyclones like Amphan typically develop a well-defined eye, where subsidence dominates and the air tends to be drier, particularly around the 700 hPa level. The presence of this dry air in the eye and surrounding regions may further reduce QV at 700 hPa, thereby reinforcing the inverse relationship between QV_700 and MSW during peak intensity phases.

In the case of Bulbul, the correlation structure is very similar to that of Amphan, except QV_700. The correlation between QV_700 and MSW is positively correlated (r = 0.5) and negatively correlated with

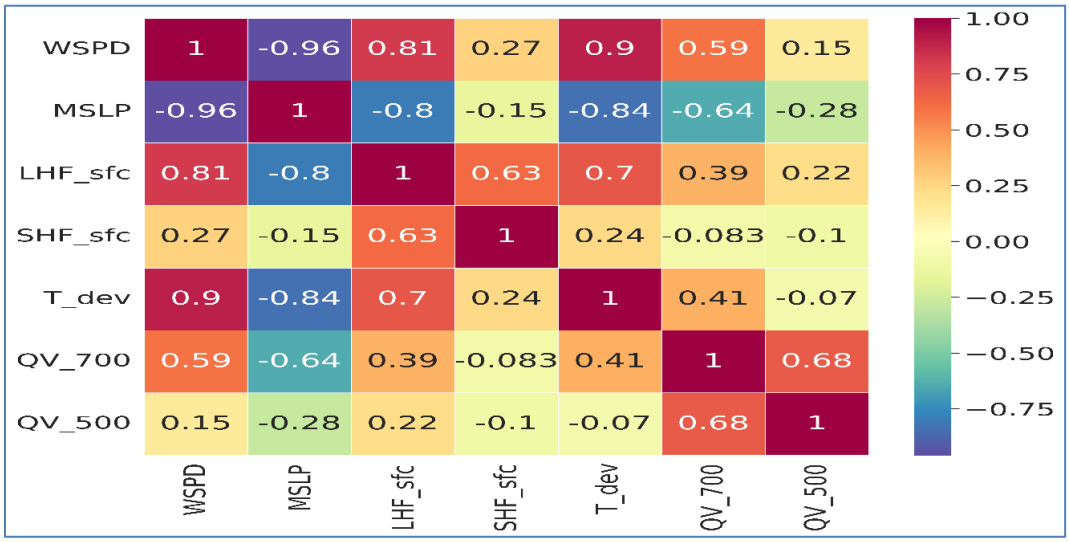

Fig. 13. Heat map representing the correlation matrix of different parameters of Titli

minimum MSLP (r = -0.62), more evident than at QV_500, pointing to the greater role of lower-tropospheric moisture in maintaining convection in this TC. LHF_sfc shows a consistent positive correlation with MSW, confirming the thermodynamic role of surface fluxes even in a less intense system. Mean T_dev deviation also demonstrates a strong positive correlation with MSW (r = 0.93), but more strongly than in Amphan. The negative correlation between minimum MSLP and the thermodynamic variables aligns with expectations of QV_700.

The heat map for Titli demonstrates a pattern similar to Amphan but with slight differences in magnitude and sensitivity. LHF_sfc and T_dev is strongly correlated with MSW (r = 0.81 and r = 0.9, respectively), reflecting the role of surface moisture fluxes and mid-level humidity in enhancing vertical motion and intensification. A particularly notable feature in Titli is the relatively strong correlation between QV_700 and MSW as compared to QV_500. As with the other TCs, minimum MSLP is negatively correlated with the thermodynamic fields, confirming the expected inverse relationship. The strong thermodynamic signal, particularly in T_dev and LHF_sfc, highlights the effectiveness of these variables as predictors of TC intensity during Titli's rapid intensification.

4. Conclusions

This study presents a comprehensive assessment of the thermodynamic processes influencing TC intensity over the BoB, with a focus on latent and sensible heat fluxes, warm core structures, and their linkages to storm evolution. Using the WRF model initialized with GDAS/FNL data, we simulated three major TCs: Amphan (2020), Bulbul (2019), and Titli (2018), and validated model outputs against ERA5 reanalysis and RSMC, New Delhi best track datasets. The WRF model showed strong skill in capturing storm structure, intensity, and thermodynamic characteristics, particularly during rapid intensification phases.

Among the three cases, Amphan reached the highest intensity, attaining SuCS status with a peak MSW of 135 knots and a minimum MSLP of 920 hPa. Bulbul and Titli, by contrast, peaked as VSCS with MSWs of 75–80 knots. A key distinction was the intensity and depth of the warm core of Amphan. WRF simulations and ERA5 both identified a warm core anomaly >8°C near 200–300 hPa for Amphan, with vertical extension up to 200 hPa, signifying strong latent heat release and deep organized convection. Bulbul and Titli exhibited shallower warm cores, with weaker anomalies (~7°C), correlating with their lower intensities.

Correlation analyses underscored the dominant role of thermodynamic factors in storm intensification. Latent Heat Flux (LHF) showed a strong positive correlation with MSW (r > 0.85) and a negative correlation with MSLP, confirming its critical role in fueling convection. Sensible Heat Flux (SHF) also contributed positively but had less impact on the weaker storms, likely due to lower air-sea thermal contrast. Upper-tropospheric temperature deviation (700–200 hPa) displayed a consistent inverse correlation with MSLP, highlighting its relevance as a proxy for cyclone maturity. Interestingly, mid-level (700 hPa) specific humidity showed a negative correlation with MSW in Amphan, possibly due to vertical ascent and eye subsidence causing mid-level drying. In contrast, Bulbul

and Titli showed positive correlations, reflecting weaker vertical mixing and more humid mid-levels.

A key finding relates to the differences in warm core representation between WRF and ERA5. For Amphan, both WRF simulations and ERA5 reanalysis consistently captured a strong and deep warm core structure, with temperature anomalies exceeding 8°C near 200-300 hPa, aligning well with its observed SuCS intensity. However, for Bulbul and Titli, ERA5 significantly underestimated the warm core strength and vertical extent compared to WRF, particularly during periods of rapid intensification. These underestimations in ERA5 likely result from its coarser resolution and smoother representation of convective processes. This contrast underscores the limitations of reanalysis data in resolving the thermodynamic structure of moderately intense cyclones and highlights the superior capability of high-resolution, physics-based models like WRF in capturing the vertical thermal structure essential for accurate intensity prediction.

In summary, the study reveals both shared thermodynamic mechanisms and storm-specific variations in cyclone intensification over the BoB. The results emphasize the need for high-resolution modeling and vertical thermodynamic profiling to improve intensity forecasts. Future research should incorporate detailed moisture diagnostics and coupled ocean-atmosphere processes to capture rapid intensification dynamics better and enhance prediction accuracy.

Acknowledgments

The authors express gratitude to NCEP/NCAR for generously providing GDAS data. Special recognition is owed to the dedicated developers of the WRF model, without whose contributions this study would not have been feasible. The authors extend sincere appreciation to RSMC, New Delhi, and ECMWF for making their data sources available. Additionally, the authors wish to acknowledge colleagues for their valuable input and suggestions throughout the study.

Authors' contributions

Kh. Hafizur Rahman: Conceptualization, analysis, writing and editing. (*email: rs77_hafizbmd@yahoo.com)*
M. A. Taher: Review and supervision. (*email: tahermath@duet.ac.bd*)

Disclaimer: The contents and views presented in this research article/paper are the views of the authors and do not necessarily reflect the views of the organizations they belong to.

References

Andersen, T.K. and Shepherd, J.M., 2014, "A global spatiotemporal analysis of inland tropical cyclone maintenance or intensification", *Int. J. Climatol*., 34, 391-402. https://doi.org/10.1002/joc.3693.

Chandrasekar, R. and Balaji, C., 2016, "Impact of physics parameterization and 3DVAR data assimilation on prediction of tropical cyclones in the Bay of Bengal region", *Natural Hazards*, 80, 223-247. doi:10.1007/s11069-015-1966-5.

Chen, X., and Zhang, F., 2017, "The role of warm-core structure in tropical cyclone rapid intensification in a high-resolution simulation", Journal of the Atmospheric Sciences, 74(4), 1275-1292, DOI: 10.1175/JAS-D-16-0158.1.

Dulac, W., Cattiaux, J., Chauvin, F., Bourdin, S., and Fromang, S. (2022). How Realistic are Tropical Cyclones in the ERA5 Reanalysis? EGU General Assembly 2022, Vienna, Austria (23-27 May 2022), EGU22-5755t, https://doi.org/10.5194/egusphere-egu22-5755.

Gopalakrishnan, S. G., Marks, F., Zhang, J. A., Zhang, X., Bao, J. W. and Tallapragada, V., 2013, "A study of the impacts of vertical diffusion on the structure and intensity of the tropical cyclones using the high-resolution HWRF system", J Atmos Sci, 70, 524-541, DOI: 10.1175/JAS-D-11-0340.1.

Komaromi, W.A. and Doyle, J. D., 2017, "Tropical Cyclone Outflow and Warm Core Structure as Revealed by HS3 Dropsonde Data", *Monthly Weather Review*, 145(4), 1339-1359, DOI:10.1175/MWR-D-16-0172.1.

Mahala, B.K., Mohantyb, P.K., Dasa, M. and Routray, A., 2019, "Performance assessment of WRF model in simulating the very severe cyclonic storm "TITLI" in the Bay of Bengal: A case study", *Dynamics of Atmospheres and Oceans*, 88, 101106, https://doi.org/10.1016/j.dynatmoce.2019.101106.

Mahala, B.K., Mohanty, P.K. and Nayak, B.K., 2015a, "Impact of microphysics schemes in the simulation of cyclone Phailin using WRF model", *Procedia Eng*, 116, 655-662, https://doi.org/10.1016/j.proeng.2015.08.342.

Mondal, M., Biswas, A., Haldar, S., Mandal, S., Bhattacharya, S. and Paul, S., 2022, "Spatio-temporal behaviors of tropical cyclones over the Bay of Bengal Basin in last five decades", *Tropical Cyclone Research and Review*, 11(1), 1-15, https://doi.org/10.1016/j.tcrr.2021.11.004.

Mugume, I., Waiswa, D., Mesquita, M.D.S., Reuder, J., Basalirwa, C., Bamutaze, Y., Twinomuhangi, R., Tumwine, F., Otim, J.S., Ngailo, T.J. and Ayesiga, G., 2017, "Assessing the performance of WRF model in simulating rainfall over western Uganda", *J Climatol Weather Forecast*, 05, 1-9, doi:10.4172/2332-2594.1000197.

Ohno, T., Satoh, M. and Yamada, Y., 2016, "Warm Cores, eyewall slopes, and intensities of tropical cyclones simulated by a 7-km-mesh global nonhydrostatic model", *Journal of Atmospheric Science*, 73, 4289-4309. doi: 10.1175/JAS-D-15-0318.1.

Osuri, K.K., Mohanty, U.C., Routray, A., Mohapatra, M. and Niyogi, D, 2013, "Real-time track prediction of tropical cyclones over the North Indian Ocean using the ARW model", *J Appl Meteorol Climatol*, 52, 2476-2492, https://doi.org/10.1175/JAMC-D-12-0313.1.

Osuri, K.K., Routray, A., Mohanty, U.C., Mohapatra, M., Kulkarni, M.A., 2011, "Customization of WRF-ARW model with physical parameterization schemes for the simulation of tropical

cyclones over North Indian Ocean", *Nat Hazards*, 63, 1337–1359, https://doi.org/10.1007/s11069-011-9862-0.

Plotnik, T., Price, C., Saha, J. and Guha, A., 2021, "Transport of Water Vapor from Tropical Cyclones to the Upper Troposphere", *Atmosphere*, 12, 1506, https://doi.org/10.3390/atmos12111506.

Raju, P.V.S., Bhatla, R., and Mohanty, U.C., 2012, "Structure and characteristics of the tropical cyclone warm core as observed from Microwave Sounding Unit (MSU)", *Journal of Geophysical Research: Atmospheres*, 117(D2), D02108, DOI: 10.1029/2011JD016574.

Reddy, M.V., Prasad, S.B.S., Krishna, U.V.M. and Reddy, K.K., 2014, "Effect of cumulus and microphysical parameterizations on the JAL cyclone prediction", *Indian J Radio Sp Phys*, 43, 103-123.

Routray, A., Dutta, D. and George, J.P., 2019, "Evaluation of track and intensity prediction of tropical cyclones over north Indian ocean using NCUM global model", *Pure Appl Geophys*, 176, 421-440, https://doi.org/10.1007/s00024-018-1924-8.

Singh, K.S., Kishtawal, C.M. and Pal, P.K., 2021, "Diagnostic analysis of the warm core and its relation to intensity changes in severe cyclonic storms over the Bay of Bengal", *Dynamics of Atmospheres and Oceans*, 93, 101206, doi:10.1016/j.dynatmoce.2021.101206.

Skamarock, W. C., Klemp, J. B., Gill, D. O., Barker, D. M., Duda, M. G., Wang, W. and Powers, J. G., 2019, "A Description of the Advanced Research WRF Version 4".

Srinivas, C.V., Bhaskar Rao, D.V., Yesubabu, V., Baskaran, R. and Venkatraman, B., 2013, "Tropical cyclone predictions over the Bay of Bengal using the high-resolution advanced research weather research and forecasting (ARW) model", *Q J R Meteorol Soc.*, 139, 1810-1825. https://doi.org/10.1002/qj.2064.

Super Cyclonic Storm "AMPHAN" over Southeast Bay of Bengal (16 May - 21 May 2020): A Report, RSMC, New Delhi, 2021

Tiwari, G., Kumar, S., Routray, A., Panda, J. and Jain, I., 2019, "A high-resolution mesoscale model approach to reproduce super typhoon Maysak (2015) over northwestern Pacific Ocean", *Earth Syst Environ*, 3, 101-112, https://doi.org/10.1007/s41748-019-00086-0.

Very Severe Cyclonic Storm "BULBUL" over the Bay of Bengal (05th - 11th November 2019): A Report, RSMC, New Delhi, 2020

Very Severe Cyclonic Storm, "TITLI" over Eastcentral Bay of Bengal (08-13 October 2018): A Report, RSMC, New Delhi, 2019

Wang, X. and Jiang, H., 2019, "A 13-year global climatology of tropical cyclone warm-core structures from AIRS data", *Monthly Weather Review*, 147, 773-790, DOI: 10.1175/MWR-D-18-0276.1

Wang, X., Jiang, H., Zhang, J.A. and Peng, K., 2020, "Satellite-observed warm-core structure in relation to tropical cyclone intensity change", *Atmospheric Research*, 240, 104931, https://doi.org /10.1016/ j.atmosres.2020.104931.